

$$T_d(R) = \begin{cases} 1, & R < R_{\min} \\ \frac{R_{\max} - R}{R_{\max} - R_{\min}}, & R_{\min} \leq R \leq R_{\max} \\ 0, & R_{\max} < R \end{cases} \quad (20)$$

4.3 Task priority

4.3.1 IT2FLS with hierarchical structure

Fig. 6 is a decision tree of radar task priority assignment. Wang (1999) pointed out that a fuzzy logic system with hierarchical structure can effectively reduce the number of fuzzy rules. Assume that a fuzzy logic system has n input variables, and each input variable has m fuzzy values. When the hierarchical structure is not adopted, the number of fuzzy rules is m^n . When using a hierarchical structure, the number of fuzzy rules is $(n-1)m^2$. The number of fuzzy rules changes from an exponential function of the input variable to a linear function of the input variable, so the rule explosion problem can be effectively solved.

Fig. 7 shows the number of fuzzy rules with different structures. When the fuzzy logic system has 5 input variables and each input variable has 3 fuzzy values, compared with a fuzzy logic system without hierarchical structure, the use of the fuzzy logic system designed in this paper reduces the number of fuzzy rules by 207 (about 85.2%). When the fuzzy logic system has 5 input variables and each input variable has 5 fuzzy values, compared with a fuzzy logic system without hierarchical structure, the use of the fuzzy logic system designed here reduces the

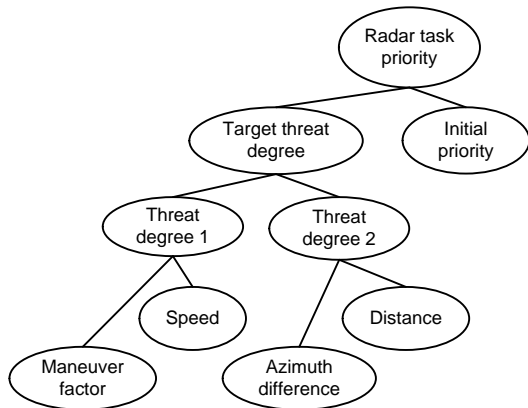


Fig. 6 Decision tree of priority assignment

number of fuzzy rules by 3025 (about 96.8%).

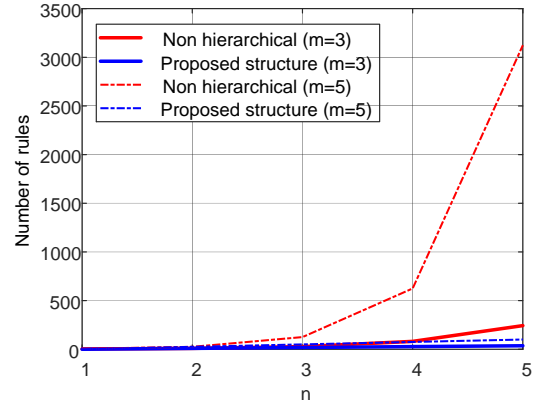


Fig. 7 Number of fuzzy rules

4.3.2 IT2FLS of radar task priority

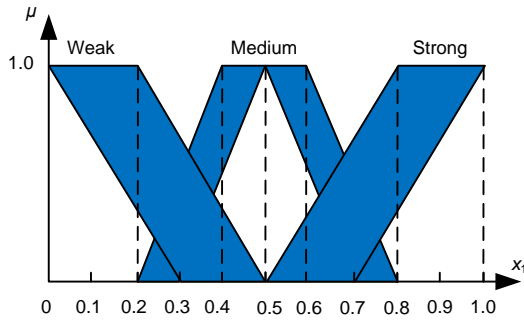
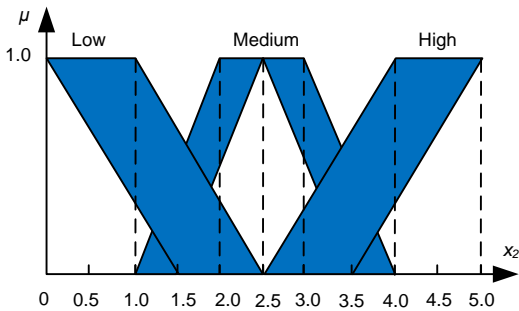
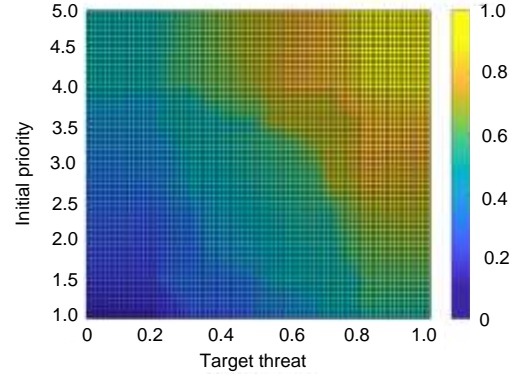
Take a fuzzy subsystem composed of a target threat degree, initial priority and radar task priority as an example. The target threat degree and initial priority are the inputs of the fuzzy subsystem and the radar task priority is the output. Table 1 shows the fuzzy variables and fuzzy values of the fuzzy subsystem. The target threat degree is the input x_1 , the initial priority is the input x_2 and the radar task priority is the output y . The fuzzy values of x_1 are \tilde{X}_{11} , \tilde{X}_{12} and \tilde{X}_{13} . The fuzzy values of x_2 are \tilde{X}_{21} , \tilde{X}_{22} and \tilde{X}_{23} . The fuzzy values of y are \tilde{G}^1 , \tilde{G}^2 , \tilde{G}^3 , \tilde{G}^4 and \tilde{G}^5 . The rule base is shown in Table 2. As shown in Fig. 8, the FOU_s of \tilde{X}_{11} , \tilde{X}_{12} and \tilde{X}_{13} are represented by nine-point vectors, which are (0.0, 0.0, 0.2, 0.5, 0.0, 0.0, 0.0, 0.3, 1.0), (0.2, 0.4, 0.6, 0.8, 0.3, 0.5, 0.5, 0.7, 1.0) and (0.5, 0.8, 1.0, 1.0, 0.7, 1.0, 1.0, 1.0, 1.0). As shown in Fig. 9, the FOU_s of \tilde{X}_{21} , \tilde{X}_{22} and \tilde{X}_{23} are represented by nine-point vectors: (0.0, 0.0, 1.0, 2.5, 0.0, 0.0, 0.0, 1.5, 1.0), (1.0, 2.0, 3.0, 4.0, 1.5, 2.5, 2.5, 3.5, 1.0) and (2.5, 4.0, 5.0, 5.0, 3.5, 5.0, 5.0, 5.0, 1.0). The membership functions of consequents of rules are respectively $\mu_{\tilde{G}^1(y)} = 1/[0, 0.2]$, $\mu_{\tilde{G}^2(y)} = 1/[0.2, 0.4]$, $\mu_{\tilde{G}^3(y)} = 1/[0.4, 0.6]$, $\mu_{\tilde{G}^4(y)} = 1/[0.6, 0.8]$ and $\mu_{\tilde{G}^5(y)} = 1/[0.8, 1]$. Fig. 10 is the crisp output of radar task priority.

Table 1 Fuzzy variables and fuzzy values

Fuzzy variable	Fuzzy value
Target threat degree (x_1)	\tilde{X}_{11} (Weak), \tilde{X}_{12} (Medium), \tilde{X}_{13} (Strong)
Initial priority (x_2)	\tilde{X}_{21} (Low), \tilde{X}_{22} (Medium), \tilde{X}_{23} (High)
Radar task priority (y)	\tilde{G}^1 (Low), \tilde{G}^2 (Medium-Low), \tilde{G}^3 (Medium), \tilde{G}^4 (Medium-High), \tilde{G}^5 (High)

Table 2 Fuzzy rule base

Rule no.	IF		THEN
	x_1	x_2	y
\tilde{R}_Z^1	\tilde{X}_{11}	\tilde{X}_{21}	\tilde{G}^1
\tilde{R}_Z^2	\tilde{X}_{11}	\tilde{X}_{22}	\tilde{G}^2
\tilde{R}_Z^3	\tilde{X}_{11}	\tilde{X}_{23}	\tilde{G}^3
\tilde{R}_Z^4	\tilde{X}_{12}	\tilde{X}_{21}	\tilde{G}^2
\tilde{R}_Z^5	\tilde{X}_{12}	\tilde{X}_{22}	\tilde{G}^3
\tilde{R}_Z^6	\tilde{X}_{12}	\tilde{X}_{23}	\tilde{G}^4
\tilde{R}_Z^7	\tilde{X}_{13}	\tilde{X}_{21}	\tilde{G}^3
\tilde{R}_Z^8	\tilde{X}_{13}	\tilde{X}_{22}	\tilde{G}^4
\tilde{R}_Z^9	\tilde{X}_{13}	\tilde{X}_{23}	\tilde{G}^5

**Fig. 8 The FOU of fuzzy value for target threat degree****Fig. 9 The FOU of fuzzy value for initial priority****Fig. 10 The crisp output of radar task priority**

5 Simulation verification and analysis

5.1 Experiment parameter settings

To verify the performance of the proposed priority assignment method, the following experiments were designed. The priority assignment methods of Lu et al. (2006) and Guo et al. (2013) were selected and marked as Method 1 and Method 2, respectively, to compare with our proposed method. The simulation experiment parameters were set as follows. Taking the hypersonic common aero vehicle (CAV-H) as an example (Duan et al., 2010), 100 batches of targets with random initial speeds and initial positions were generated (Li et al., 2017). The radar position was (1500, 0, -0.1) km, the radar operating frequency was $f_r=433$ MHz, the transmit and receive gain was $G=41$ dB, the radar transmit peak power was $P_t=1164$ kW, and the radar duty cycle was 25%. The RCS of the target was $RCS=0.1$ m², the target detection probability was $P_d=0.9$, and the false alarm rate was $P_{fa}=1 \times 10^{-6}$.

The trajectory of the partial targets is shown in Fig. 11. Fig. 12 shows the flight speed of the HGVs. Fig. 13 shows the distance between the HGVs and the radar. Fig. 14 shows the azimuth difference between the HGVs and the radar.

Table 3 shows the initial priority, dwell time, time window and period of the radar tasks. The length of the scheduling interval was $SI_i=50$ ms, and the total number of scheduling intervals was $M=200$. $V_{max}=7900$ m/s, $V_{min}=1700$ m/s, $R_{max}=1200$ km, $R_{min}=200$ km, $\Delta\chi_{max}=180^\circ$, $\Delta\chi_{min}=-180^\circ$. Figs. 15 and 16 show the FOU of the fuzzy values for the maneuver factor and flight speed, respectively. Fig. 17

shows the crisp output of threat degree 1. Figs. 18 and 19 show the FOUs of the fuzzy values for the distance between the HGV and the radar and the azimuth difference between the HGV and the radar, respectively. Fig. 20 shows the crisp output of threat degree 2.

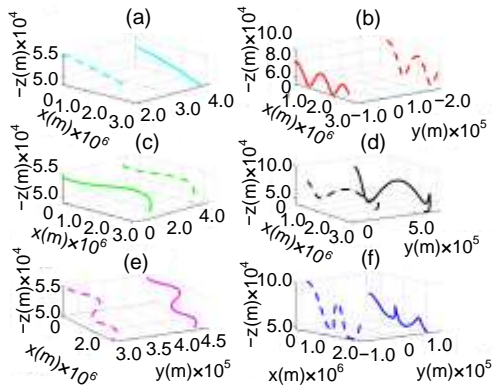


Fig. 11 The ballistic trajectory of the HGVs

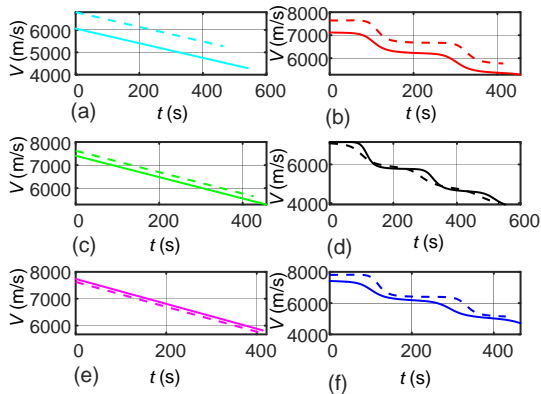


Fig. 12 The flight speed of the HGVs

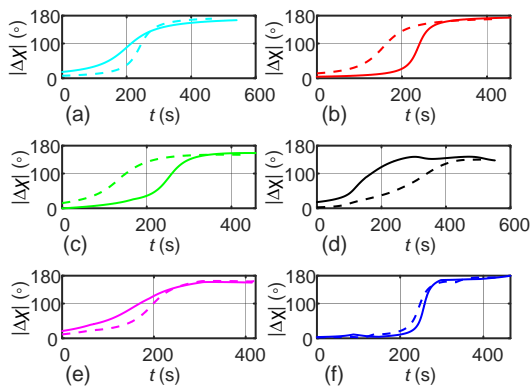


Fig. 13 The azimuth difference between the HGVs and the radar

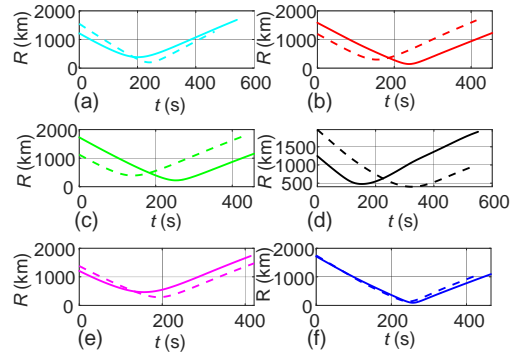


Fig. 14 The distance between the HGVs and the radar

Table 3 Radar task parameters

Task type	Initial priority	Dwell time (ms)	Time window (ms)	Task cycle (ms)
Confirmation	5	7	30	-
Precise tracking	4	5	30	500
Tracking loss	3	7	40	-
Normal tracking	2	8	50	1000
Search	1	9	100	2000

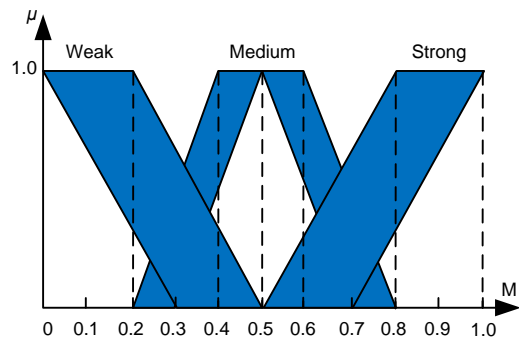


Fig. 15 The FOU of the fuzzy value for maneuver factor

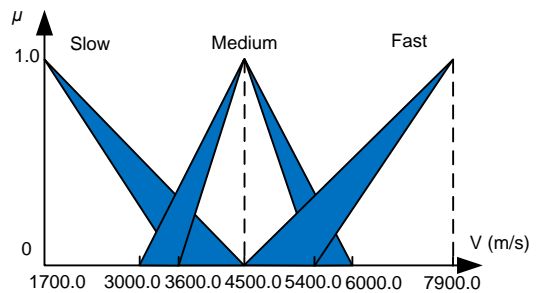


Fig. 16 The FOU of the fuzzy value for speed

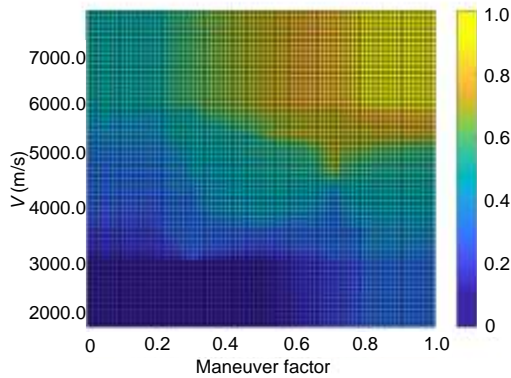


Fig. 17 The crisp output of threat degree 1

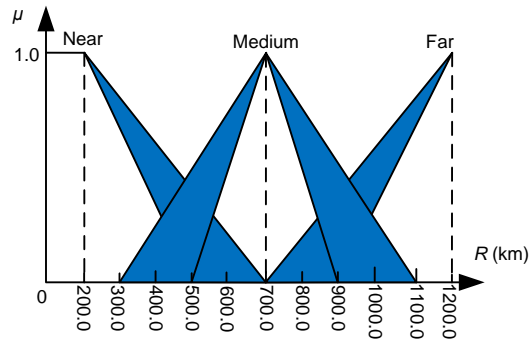


Fig. 18 The FOU of the fuzzy value for distance

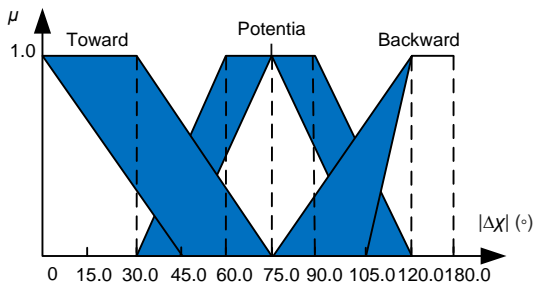


Fig. 19 The FOU of the fuzzy value for azimuth difference

5.2 Analysis of experimental results

The Fig. 21 shows the length of the remaining time slices in each scheduling interval of the three methods under the condition of 96 batches of target. The remaining time slices were all less than 2.8 ms and it was no longer possible to schedule more radar tasks in each scheduling interval. The three methods made full use of the time resources of each scheduling interval.

The Fig. 22 shows part of the task scheduling results of the three methods (Fig. 22a, method 1; Fig. 22b, method 2; Fig. 22c, our proposed method) under the condition of 96 batches of target. When radar task

priority assignment was carried out using our proposed method, the number of high initial priority tasks successfully scheduled was obviously greater than those scheduled by methods 1 or 2.

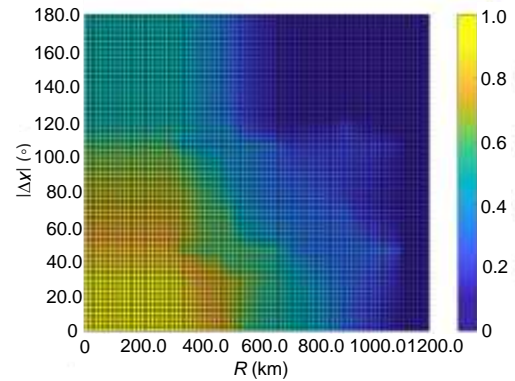


Fig. 20 The crisp output of threat degree 2

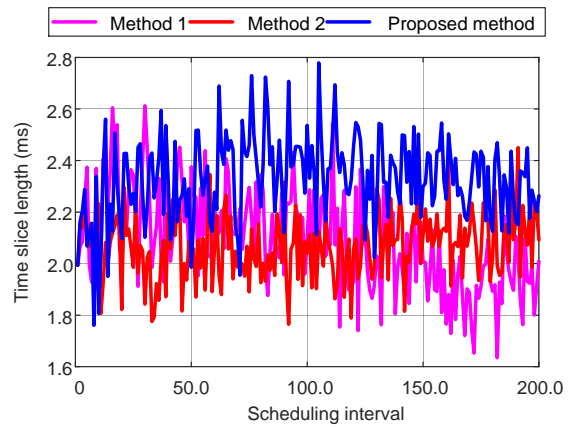


Fig. 21 The length of the remaining time slices in each scheduling interval

5.2.1 Initial priority

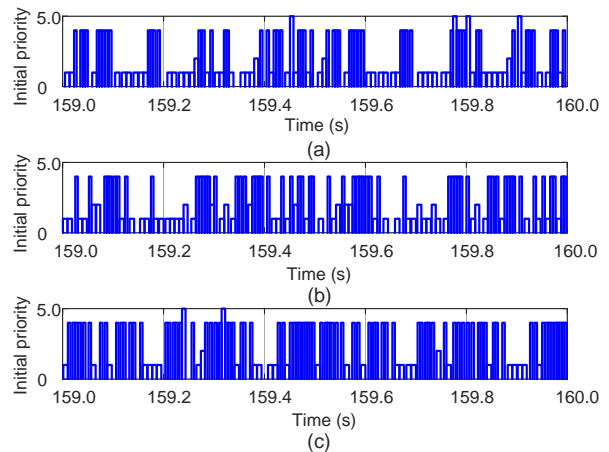


Fig. 22 The task scheduling results of the three methods

Fig. 23 shows the mean initial priority of radar tasks in the execution queue. As the number of targets increased, the mean initial priorities of the radar tasks in the execution queue of the three methods showed an increasing trend. When the radar task priorities were assigned by our proposed method, the mean initial priority of the radar task in the execution queue was the highest. When the number of targets was greater than 50 batches, the mean initial priority of our proposed method was about 21.3% higher than that of method 1, and about 16.5% higher than that of method 2.

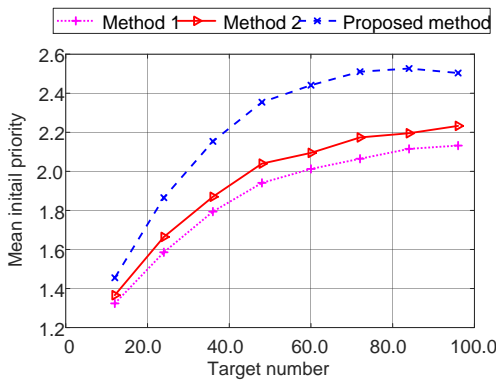


Fig. 23 The mean initial priority of radar tasks in the execution queue

Fig. 24 shows the mean initial priority of radar tasks in the deleted queue. With the increase in the number of targets, the mean initial priority of the radar tasks in the deleted queue showed an increasing trend. When using our proposed method to assign the radar task priorities, the mean initial priority of the radar task in the deleted queue was the lowest. When

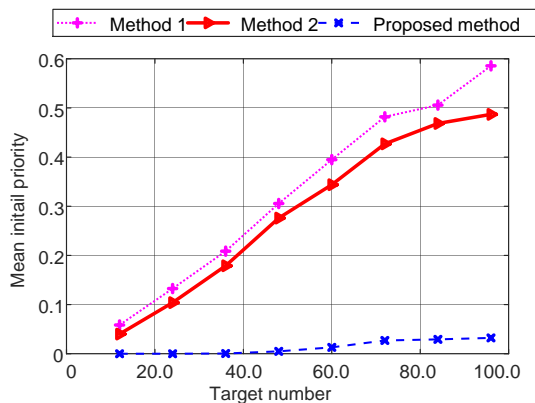


Fig. 24 The mean initial priority of radar tasks in the deleted queue

the number of targets was greater than 70 batches, the mean initial priority of radar tasks in the deleted queue of our proposed method was significantly lower than those of methods 1 and 2.

5.2.2 Target threat degree

Fig. 25 shows the maneuver threat of radar tasks in the execution queue. As the number of targets increased, the maneuver threats of the three methods also increased. When the radar task priorities were assigned by our proposed method, the radar tasks had the greatest maneuver threat. When the number of targets was greater than 50 batches, the maneuver threat of our proposed method was about 40.3% higher than that of method 1, and 28.8% higher than that of method 2.

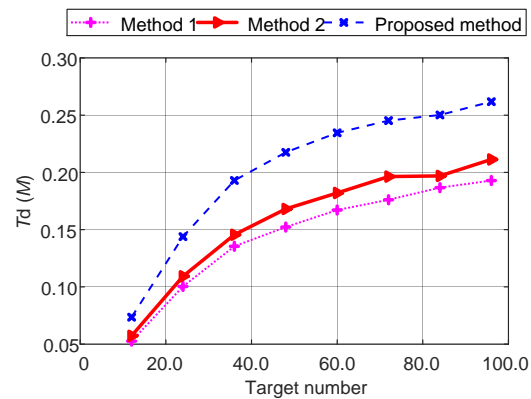


Fig. 25 Maneuver threat of the radar tasks

Fig. 26 shows the speed threat of radar tasks in the execution queue. As the number of targets increased, the speed threats of the three methods all showed an upward trend. When the radar task priorities were assigned by our proposed method, the speed

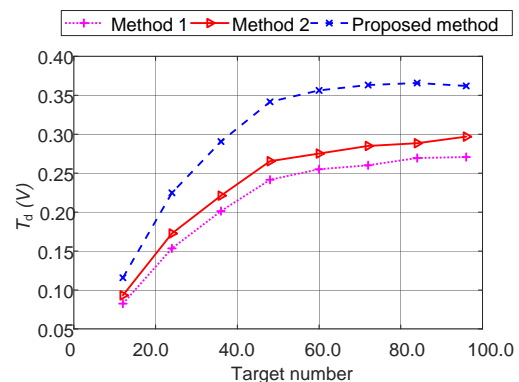


Fig. 26 Speed threat of the radar tasks

threat of the radar tasks was the highest. When the number of targets was greater than 50 batches, the speed threat of our proposed method was about 39.6% higher than that of method 1, and 27.4% higher than that of method 2.

Fig. 27 shows the azimuth threat of radar tasks in the execution queue. As the number of targets increased, the azimuth threats of the three methods all showed an upward trend. When the radar task priorities were assigned by our proposed method, the azimuth threat of the radar task was the highest. When the number of targets was greater than 50 batches, the azimuth threat of our proposed method was about 38.2% higher than that of method 1, and 26.1% higher than that of method 2.

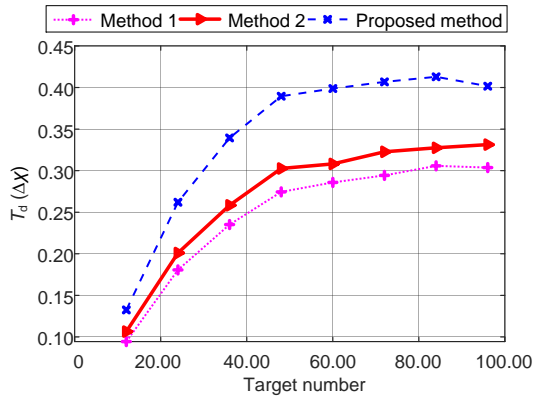


Fig. 27 Azimuth threat of the radar tasks

Fig. 28 shows the distance threat of radar tasks in the execution queue. As the number of targets increased, the distance threats of the three methods all showed an upward trend. When using our proposed method to assign priorities of radar tasks, the distance threat of radar tasks was the highest. When the number of targets was greater than 50 batches, the distance threat of our proposed method was about 42.3% higher than that of method 1, and 30.2% higher than that of method 2.

5.2.3 Search rate and precise tracking rate

Fig. 29 shows the search rate of the radar tasks. As the number of targets increased, the radar task search rates of the three methods all showed a downward trend. When the radar task priority was assigned by our proposed method, the search rate of

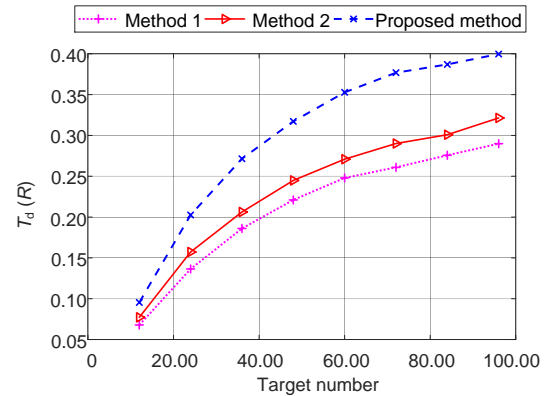


Fig. 28 Distance threat of the radar tasks

the radar tasks was the lowest. When the targets were less than 48 batches, the search rates of the three methods were all higher than 50%, but the search rate of our proposed method was the lowest. When the targets were greater than 60 batches, the search rate of our proposed method dropped below 50%, which is about 14.3% lower than that of method 1, and about 11.1% lower than that of method 2.

Fig. 30 shows the precise tracking rate of the radar tasks. As the number of targets increased, the precise tracking rates of the three methods showed an upward trend. When the radar task priorities were assigned by our proposed method, the precise tracking rate of the radar tasks was the highest. When the targets were less than 36 batches, the precise tracking rates of the three methods was less than 40%, and the precise tracking rate of our proposed method was the highest. When the targets were larger than 48 batches, the precise tracking rate of our proposed method rose to more than 40%, which is about 14.8% higher than that of method 1, and about 10.8% higher than that of method 2.

5.2.4 Offset time and scheduling success rate

Fig. 31 shows the offset between the actual execution time of the radar tasks and the expected execution time. As the number of targets gradually increased, the offset time of the three methods all showed a downward trend. As the number of targets increased, the number of precise tracking radar tasks increased accordingly. The dwell time and time window of precise tracking tasks were the shortest among all radar tasks, so the offset time of radar tasks showed a gradual decline. When the targets were greater than 60 batches, the offset time of our pro-

posed method was about 22.8% lower than that of method 1, and about 10.5% lower than that of method 2.

Fig. 32 shows the scheduling success rate of radar tasks. The scheduling success rates of the three methods did not show a significant upward or downward trend with the increase in the number of incoming targets. The scheduling success rates of the three methods basically remained stable, from 83–85%.

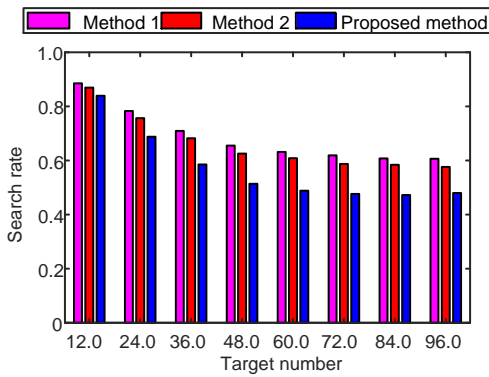


Fig. 29 Search rate of the radar tasks

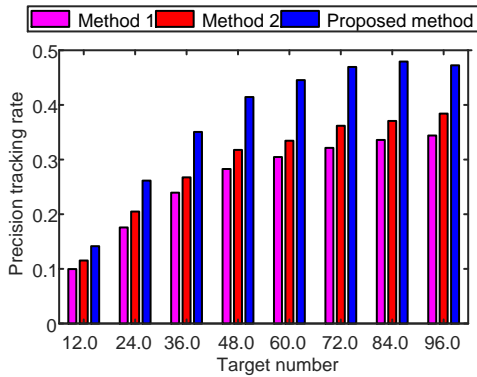


Fig. 30 Precise tracking rate of the radar tasks

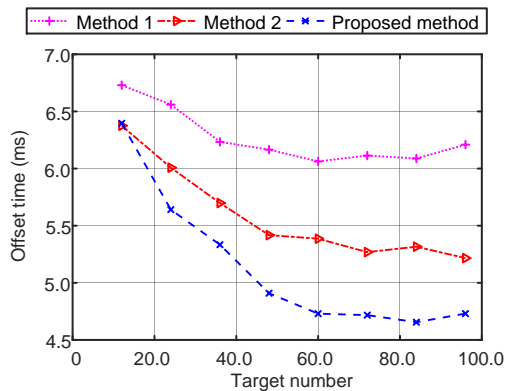


Fig. 31 Offset time of the radar tasks

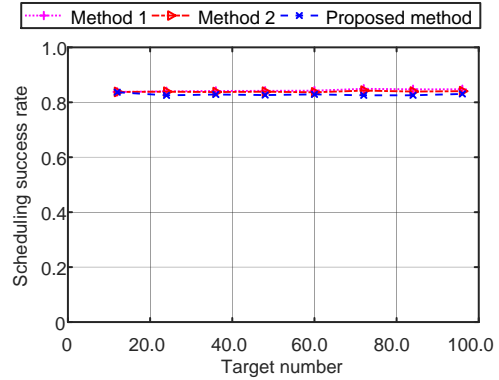


Fig. 32 Scheduling success rate of the radar tasks

6 Conclusions

In this research we designed a task priority assignment method based on IT2FLS with the aim of alleviating the radar resource management problem when ground-based phased-array radar detects HGVs in near space. Compared with method 1 and method 2, the method proposed in this paper has stronger information perception ability and can effectively screen radar tasks with high threat and high initial priority. When the targets were greater than 50 batches, the mean initial priority, target threat degree, and precise tracking rate were significantly higher than those of methods 1 and 2. While maintaining a scheduling success rate equivalent to those of methods 1 and 2, the task offset time of our proposed method was significantly lower.

In future work, it is necessary to study the robustness of IT2FLS and analyze the influence of the FOU of the fuzzy value on the performance of IT2FLS. It will also be necessary to analyze the influence of the number of fuzzy rules on the performance of IT2FLS, and study how to effectively reduce the number of fuzzy rules while ensuring the system performance does not decrease, thereby reducing the complexity of system design.

Contributors

Fanqing MENG designed the research, processed the data, and wrote the first draft of the manuscript. Kangsheng TIAN revised and edited the final version.

Compliance with ethics guidelines

Fanqing MENG and Kangsheng TIAN declare that they have no conflict of interest.

References

- Bao PF, Huang XP, Zhou XC, 2018. Adaptive scheduling algorithm for passive radar tasks with integrated priority. *Mod Def Technol*, 46(1):141-147, 183 (in Chinese). <https://doi.org/10.3969/j.issn.1009-086x.2018.01.023>
- Castillo O, Cervantes L, Soria J, et al., 2016a. A generalized type-2 fuzzy granular approach with applications to aerospace. *Inf Sci*, 354:165-177. <https://doi.org/10.1016/j.ins.2016.03.001>
- Castillo O, Amador-Angulo L, Castro JR, et al., 2016b. A comparative study of type-1 fuzzy logic systems, interval type-2 fuzzy logic systems and generalized type-2 fuzzy logic systems in control problems. *Inf Sci*, 354:257-274. <https://doi.org/10.1016/j.ins.2016.03.026>
- Castillo O, Melin P, Ontiveros E, et al., 2019. A high-speed interval type 2 fuzzy system approach for dynamic parameter adaptation in metaheuristics. *Eng Appl Artif Intell*, 85:666-680. <https://doi.org/10.1016/j.engappai.2019.07.020>
- Cervantes L, Castillo O, 2015. Type-2 fuzzy logic aggregation of multiple fuzzy controllers for airplane flight control. *Inf Sci*, 324:247-256. <https://doi.org/10.1016/j.ins.2015.06.047>
- Ding Z, Moo P, 2017. Benefits of target prioritization for phased array radar resource management. Proc 18th Int Radar Symp, p.1-7. <https://doi.org/10.23919/IRS.2017.8008153>
- Duan GR, Sun Y, Zhang MR, et al., 2010. Aerodynamic coefficients models of hypersonic vehicle based on aero database. Proc 1st Int Conf on Pervasive Computing, Signal Processing and Applications, p.1001-1004. <https://doi.org/10.1109/PCSPA.2010.247>
- Guo KP, Zuo Y, Xue AK, 2013. An Adaptive Task scheduling algorithm based on the fuzzy logic priority for multi-function radars. *J Jiangnan Univ (Nat Sci Ed)*, 12(5): 591-595 (in Chinese). <https://doi.org/10.3969/j.issn.1671-7147.2013.05.015>
- Jiménez MI, del Val L, Villacorta JJ, et al., 2012. Design of task scheduling process for a multifunction radar. *IET Radar Sonar Navig*, 6(5):341-347. <https://doi.org/10.1049/iet-rsn.2011.0309>
- Kumar GN, Ikram M, Sarkar AK, et al., 2018. Hypersonic flight vehicle trajectory optimization using pattern search algorithm. *Optim Eng*, 19(1):125-161. <https://doi.org/10.1007/s11081-017-9367-0>
- Li B, Tian LY, Chen DQ, et al., 2020. A task scheduling algorithm for phased-array radar based on dynamic three-way decision. *Sensors*, 20(1):153. <https://doi.org/10.3390/s20010153>
- Li GH, Zhang HB, Tang GJ, 2015. Maneuver characteristics analysis for hypersonic glide vehicles. *Aerosp Sci Technol*, 43:321-328. <https://doi.org/10.1016/j.ast.2015.03.016>
- Li GH, Zhang HB, Tang GJ, 2017. Flight-corridor analysis for hypersonic glide vehicles. *J Aerosp Eng*, 30(1):06016005. [https://doi.org/10.1061/\(ASCE\)AS.1943-5525.0000667](https://doi.org/10.1061/(ASCE)AS.1943-5525.0000667)
- Lu JB, Hu WD, Yu WX, 2006. Study on real-time task scheduling of multifunction phased array radars. *Acta Electron Sin*, 34(4):732-736 (in Chinese). <https://doi.org/10.3321/j.issn:0372-2112.2006.04.032>
- Mendel JM, 2017. Uncertain Rule-based Fuzzy Systems: Introduction and New Directions. 2nd ed. Springer, Cham, Germany. <https://doi.org/10.1007/978-3-319-51370-6>
- Meng FQ, Tian KS, 2020. Analysis on influence of the bank angle of hypersonic glide vehicle. *J Astronaut*, 41(4): 419-428. <https://doi.org/10.3873/j.issn.1000-1328.2020.04.005>
- Miranda SLC, Baker CJ, Woodbridge K, et al., 2007. Fuzzy logic approach for prioritisation of radar tasks and sectors of surveillance in multifunction radar. *IET Radar, Sonar Navig*, 1(2):131-141. <https://doi.org/10.1049/iet-rsn:20050106>
- Moreno JE, Sanchez MA, Mendoza O, et al., 2020. Design of an interval type-2 fuzzy model with justifiable uncertainty. *Inf Sci*, 513:206-221. <https://doi.org/10.1016/j.ins.2019.10.042>
- Ontiveros E, Melin P, Castillo O, 2020. Comparative study of interval Type-2 and general Type-2 fuzzy systems in medical diagnosis. *Inf Sci*, 525:37-53. <https://doi.org/10.1016/j.ins.2020.03.059>
- Ontiveros-Robles E, Melin P, Castillo O, 2018. Comparative analysis of noise robustness of type 2 fuzzy logic controllers. *Kybernetika*, 54(1):175-201. <https://doi.org/10.14736/kyb-2018-1-0175>
- Wang LX, 1999. Analysis and design of hierarchical fuzzy systems. *IEEE Trans Fuzzy Syst*, 7(5):617-624. <https://doi.org/10.1109/91.797984>
- Wu DR, Mendel JM, 2019. Recommendations on designing practical interval type-2 fuzzy systems. *Eng Appl Artif Intell*, 85:182-193. <https://doi.org/10.1016/j.engappai.2019.06.012>
- Wu DR, Zeng ZG, Mo H, et al., 2020b. Interval type-2 fuzzy sets and systems: overview and outlook. *Acta Automat Sin*, 46(8):1539-1556 (in Chinese). <https://doi.org/10.16383/j.aas.c200133>
- Wu J, Lu F, Zhang JW, et al., 2020a. Design of task priority model and algorithm for imaging observation problem. *J Syst Eng Electron*, 31(2):321-334. <https://doi.org/10.23919/JSEE.2020.000010>
- Xiao S, Tan XS, Wang H, et al., 2015. Detection performance assessment of near-space hypersonic target based on ground-based radar. *J Electron Inf Technol*, 37(7):1723-1728 (in Chinese). <https://doi.org/10.11999/JEIT141024>
- Yang SC, Tian KS, Li HQ, et al., 2020. Comprehensive priority-based task scheduling algorithm for anti-missile early warning phased array radar. *Acta Armament*, 41(2): 315-323 (in Chinese). <https://doi.org/10.3969/j.issn.1000-1093.2020.02.013>
- Zhang HW, Xie JW, Lu WL, et al., 2017a. A scheduling method based on a hybrid genetic particle swarm algorithm for multifunction phased array radar. *Front Inf*

- Technol Electron Eng*, 18(11):1806-1816.
<https://doi.org/10.1631/FITEE.1601358>
- Zhang HW, Xie JW, Zong BF, et al., 2017b. Dynamic priority scheduling method for the air-defence phased array radar. *IET Radar Sonar Navig*, 11(7):1140-1146.
<https://doi.org/10.1049/iet-rsn.2016.0549>
- Zhang HW, Xie JW, Shi JP, et al., 2017c. Dynamic priority online interleaving scheduling algorithm for the air defense phased array radar. *Syst Eng Electron*, 39(3): 529-535 (in Chinese).
<https://doi.org/10.3969/j.issn.1001-506X.2017.03.11>
- Zhang HW, Xie JW, Shi JP, et al., 2018. Online interleaving scheduling algorithm over dynamic priority for the air defense phased array radar. *Acta Electron Sin*, 46(1): 55-60 (in Chinese).
<https://doi.org/10.3969/j.issn.0372-2112.2018.01.008>
- Zhang HW, Xie JW, Ge JA, et al., 2019. A hybrid adaptively genetic algorithm for task scheduling problem in the phased array radar. *Eur J Oper Res*, 272(3):868-878.
<https://doi.org/10.1016/j.ejor.2018.07.012>